RSC Advances

ROYAL SOCIETY OF CHEMISTRY

www.rsc.org/advances

A green approach for induced gelation of silk fibroin using sophorolipid to form tunable porous biomedical scaffolds

Parul Dubey[a], *Laxman Nawale*[b], *Dhiman Sarkar*[b], *Anuya Nisal*[c*], *Asmita Prabhune*[a*]

[a]Biochemical Sciences Division, [b]Combichem-Bioresource Center, OCD, [c]Polymer Science & Engineering Department, National Chemical Laboratory, Pune - 411008, India

Corresponding Authors: Asmita Prabhune, Biochemical Sciences division, National Chemical Laboratory, Pune – 411008, India. Tel.: +91 20 25902239; fax: +91 20 25902648; E-mail address: aa.prabhune@ncl.res.in

Anuya Nisal, Polymer Science and Engineering Department, National Chemical Laboratory, Pune-411008, India. Tel.: +91 20 25903013; fax: +91 20 25902648; E-mail address: aa.nisal@ncl.res.in

Abstract

Three dimensional polymer hydrogels, based on both natural and synthetic polymers, are increasingly being used as scaffolds and drug delivery vehicles for biomedical applications. Fibrous protein, silk fibroin (SF), obtained from *Bombyx mori* silkworm is a promising candidate in this area. However, SF has a long gelation time of about few weeks that can only be reduced by non-physiological treatments (e.g. high temperature, ultrasonication and low pH) or by addition of a chemical and non-biodegradable polymer and/or surfactant. We report here, accelerated gelation of SF, under physiological conditions, using a biosurfactant, sophorolipid (SL) as a gelling agent. SL and SF are completely miscible and form a very clear solution upon mixing. Hence it is interesting to see that this clear solution gels in a time span of just few hours. The hydrogels so formed have pore architecture, porosities and mechanical stability ideally suitable for tissue culture applications. Here we also demonstrate that mouse fibroblasts cells not only adhere to but also extensively proliferate on these SF-SL scaffolds.

Keywords: Silk fibroin, hydrogels, porosity, biodegradable, biosurfactants, fibroblast.

Introduction

Silk fibroin (SF) protein, derived from *Bombyx mori* silkworm, has been extensively studied in the biomedical field, due to its inherent and remarkable properties such as excellent biocompatibility, tunable biodegradability, excellent thermo-mechanical stability and minimum inflammatory reaction. SF can be processed in versatile forms such as thin films, sponges, composites, fibers, microspheres, tubes and hydrogels [1]. Polymer hydrogels are increasingly being used for biomedical applications as they give 3D porous and stable scaffolds [2]. Some attractive hydrogel-based biomedical applications include controlled drug release and tissue engineering scaffolds for the repair and regeneration of defective tissues and organs [3,4]. Biodegradable polymers are being evaluated as templates to facilitate the three dimensional culture of cells and also provide the guidance for the formation of new tissue.

SF hydrogels have been extensively studied in the last two decades. SF hydrogels can be prepared by employing non-toxic cross-linking agents such as genipin [5], which results in inter and intra covalent cross-links between SF molecules. SF hydrogels can also be prepared by physical mechanisms such as, vortexing, sonication, electrical currents and acidic pH [6–9]. Here, the gelation is driven by change in conformation of the SF molecule from random coil to beta sheet structures. Aqueous solutions of SF are extremely sensitive to the pH. The gelation of aqueous SF solution can vary from 10-16 hours (below the isoelectric pH) to a period of few days and weeks (slightly above the isoelectric pH). This long gelation time limits the clinical applications of SF [10].

Researchers have also demonstrated use of other methods to accelerate gelation of SF. Additives such as polyethylene oxide (PEO) [11] and Pluronic (Poloxamer) [12] and an anionic surfactant, sodium dodecyl sulphate (SDS) [13], have been used as gelling agents for silk fibroin under mild conditions. However, PEO (5 wt%, 60°C) reduces the gelation time in limited fashion only to approximately 9 days whereas in case of Polaxamer (15 wt%, 35°C) gelation occurs within 5 minutes. SDS at 8-12 mM concentration reduces the gelation time from few

hours to 15-18 minutes. Apart from polymers researchers have also demonstrated the use of inorganic material such as nano-silica for accelerated gelation of silk [14]. These additives are not ideal for forming biologically relevant hydrogels because of their chemical and non-biodegradable nature [13].

In the present work, we evaluate a new molecule - sophorolipid as a gelling agent for silk fibroin. Sophorolipids (SL) are carbohydrate based amphiphilic biosurfactants derived from non-pathogenic yeast *Candida bombicola*. Structurally SLs are composed of a disaccharide, sophorose (2-O-β-D-glucopyranosyl-β-D-glucopyranose) linked by non-amide polar-nonpolar linkage to hydrophobic chain of 16-18 carbons. Additional esterification step within the molecule leads to formation of two types of SLs: acidic and lactonic [15]. The hydroxyl fatty acid moiety remains free in acidic form whereas upon esterification with 4" OH group of sophorose, it converts into lactonic form. Of the two forms, acidic SL has better assembling nature and water solubility whereas the lactonic form gives SL its biological properties. Thus, optimal performance can be achieved by the mixture of these two forms.

Sodium dodecyl sulphate has been successfully used as an inducer for gelation of silk fibroin. SL has a chemical structure similar to SDS and hence it might have the potential to induce and accelerate gelation of SF through hydrophobic interactions. Also, SLs have several advantages over earlier reported gelling agents. SLs are natural compounds derived using a completely biological process. Thus, SL's have improved biocompatibility and reduced environmental impact as compared to the synthetic counterparts [16]. These biological properties have been exploited in a variety of applications including antimicrobial activity against bacteria [17], inhibition of HIV virus [18], anticancer activity [19] and ability to induce cell differentiation [20]. The dermal fibroblast metabolism stimulating activity [21] of SLs as well as increasing efficacy of topical antibiotics against microorganisms responsible for the majority of skin and soft tissue infections [22] makes them promising candidates for wound dressing application.

Thus these biological properties of SL make it an interesting gelling agent. The hydrogels of silk fibroin so formed can be used for wound dressing applications. Further, these hydrogels can be lyophilized into 3D scaffolds, which may be useful in tissue regeneration.

Here, we demonstrate that addition of SL to SF solutions results in accelerated gelation of SF near physiological pH, with gelation time reduced from few weeks to few hours. The method involves simple mixing of aqueous SF and SL solutions. We, further lyophilize these hydrogels to form three dimensional SF-SL scaffolds with controlled porosity, pore architecture and excellent mechanical properties. These lyophilized scaffolds have been evaluated for the growth and proliferation of fibroblast L929 cells, considering their future use in wound dressing applications. This is the first report showing the use of biosurfactant for the accelerated gelation of SF at near physiological pH and a provisional patent has been filed for this formulation.

Results

Gelation of silk fibroin solutions has been conventionally monitored using time sweep experiment in couette geometry in a rheometer [10,23]. We report here results on gelation of pure SF and SF-SL solutions at near physiological pH. As can be seen from Figure 1, the pure SF solution at pH 8 shows a near flat storage modulus (G′) and loss modulus (G″) during the entire experimental time frame. The SF solution does not exhibit gel-like behaviour even after storage at room temperature for a period of 20 days. When 1 w/v% SL solution is mixed with 3 w/v% SF solution, a clear solution with a pH of about 7.4 ± 0.2 is obtained. This S1 sample was then used for the rheology experiments. As shown in Figure 1, S1 shows a dominant G″ for the initial 180 minutes. However, the storage modulus rapidly builds up after 180 minutes. After 189 minutes, the G′ dominates the G″. This indicates the formation of gel. A corresponding increase in G″ is also seen at this time interval. Similar results were also observed for the SF-SL solutions with increasing concentrations of SL to 3w/v%. The gelation time was considered to be the time at which G′ and G″ had equal values and after this the G′ was always greater than G″, indicating

a solid like behaviour. The gelation time of the S3 hydrogel further decreased to 140 minutes as compared to 189 minutes for the S1 sample. But, further increasing the SL concentration did not result in further reduction of gelation time. S5 had a gelation time of about 164 minutes. Hence higher concentrations of SL were not evaluated. Figure 1 also suggests that the S5 sample has the lowest storage modulus values. The S1 and S3 have comparable modulus, but the modulus of S1 has still not reached a plateau due to slower gelation kinetics. This implies that the effective modulus of the hydrogel is essentially governed by the amount of SF present. Addition of SL negatively affects the storage modulus. However, we did not observe these trends in the wet compression modulus studies on these hydrogels. The compression modulus of the wet hydrogels was found to be of the order of ~9000Pa with no significant change with respect to formulation.

The gelation of SF is accompanied by change in conformation of the silk fibroin molecules from a predominantly random coil structure to highly crystalline beta sheet structures. To verify the same, we used Fourier Transform Infrared (FTIR) spectroscopy. FTIR is a powerful and common tool for the investigation of molecular conformations, especially in the study of silk protein structure [24]. The major conformations of SF are random coil, α-helix, β-sheets and β-turns. Sample S3 was chosen for this study and a time dependent (ATR) measurement was performed on this sample as shown in Figure 2a. The amide peak between 1600-1700 cm^{-1} was monitored and further deconvoluted to quantify the beta sheets present in the sample. The amide I peak corresponding to C=O stretching, progressively shifted to lower wavenumbers, indicating a conversion from a predominant random coil structure to crystalline beta-sheet conformation. The initial peak, corresponding to the homogenously mixed SF and SL sample centred at 1646 cm^{-1}, shifted to values of 1637, 1636 1633 and 1622 cm^{-1} after 2, 4, 6 h and 24 h respectively. The peak centred at 1646 cm^{-1} is attributed to a random coil conformation, while the peaks located in the range of 1623–1637 cm^{-1} attributed to anti-parallel beta-sheet structures [24].

Time dependent ATR-FTIR measurements of S3 sample showed an increase in β-sheet content during gelation (Figure 2b). A gradual increase in the % beta sheets in different samples was observed with increase in concentration of SL (Refer Figure 3). The S5 sample showed the highest beta sheets content at 40.4 % ±0.2 (std. error) when measured at 6h. This indicates that the concentration of SL plays a significant role in conversion of random coil to beta sheet structure. Higher the concentration of SL present, higher is the % beta sheet structure in the sample at a given time.

The three gelled samples were further frozen and lyophilized to obtain 3D porous scaffolds. Several different characterization techniques were used to evaluate the suitability of these scaffolds for cell culture experiments. First, the dry compression modulus of the lyophilized scaffolds of SF-SL was measured (Figure 4). With increasing concentration of SL from 1 to 5 w/v%, the corresponding dry compression modulus of the hydrogels decreased from 2.5 to 0.4 MPa. The SF-SL hydrogels with higher protein and lower sophorolipid content i.e. 3:1 concentration ratio had maximum compression modulus. As SF takes more than 20 days to gel, scaffolds of SF could not be prepared and hence could not be compared with the SF-SL hydrogels. However, the dry compression modulus of SF scaffolds prepared by freezing and lyophilizing have moduli in the range of few MPa, which is comparable to that obtained for our sample S1 [1]. Clearly, addition of a small organic molecule like SL deteriorates the modulus of the scaffold. However, the measured compression moduli indicate that the mechanical integrity of these 3D structures is sufficient to be evaluated for tissue engineering applications.

The cross-sectional morphology of these 3D scaffolds was visualized using a scanning electron microscope. The scaffolds represented a continuous porous morphology. A clear trend in pore size was observed i.e., with increasing SL concentration from 1 w/v % to 3 w/v % to 5 w/v %, pore size decreased from 143 ± 32 μm to 114 ± 23 μm to 32 ± 8μm respectively (Figure 5). The internal architecture of the hydrogels was dependent on SL concentration. The % porosity as calculated by liquid displacement method reported elsewhere [25] was found to be 90 ±

3% for all the scaffolds. This high porosity and large pore sizes in scaffolds is also desirable for tissue engineering applications for easy transport of nutrients and cell migration.

These scaffolds were then evaluated in cell culture studies using mouse fibroblast L929 cells. The adhesion of mouse fibroblast to the SF-SL scaffolds was characterized after 4 and 8 h (Figure 6). The porous structure of the scaffolds provides a 3D space with enhanced surface area thus increasing the available space for the cells to adhere. This was proved by higher percentage of cells attached to scaffolds in comparison to control polystyrene culture plates. Also, an increase in SL content resulted in small improvements in the ability of the cells to attach to the scaffold. Not a very significant difference in the % cell adhesion was found between the three samples, which well corroborated with the minor variation in % porosity of the scaffolds.

The cell viability was investigated at day 2, 4 and 7 by performing MTT assay (Figure 7). Short term observation (day 2) exhibited significant difference between the cells cultured within the scaffolds and control, demonstrating scaffolds lacking any adverse effect on cell growth. This indicates that the scaffold material is non-toxic. On day 4 it was observed that cells within S3 and S5 scaffolds showed significantly greater cellular activity than the control polystyrene plates. The higher cell proliferation could be attributed to the higher surface area available for cell attachment in a 3D scaffold as compared to that available in 2D culture plates. On day 7, significant difference in cellular activity as compared to the culture plate was found only in S5 scaffolds. This result clearly showed that sophorolipid does not exert any significant adverse effect on the viability of cells and higher SL proved to be even more nourishing for the increased cellular activity.

Also, confocal microscopy done on day 2 confirmed effective migration and distribution of cells within the scaffolds. The confocal images reinforced the profile obtained from MTT assay, as more profuse population of cell was found habitating within the scaffolds made of highest SL concentration (5 w/v%) (Figure 8a). Cells in S5 sample completely covered the scaffold surface, filling up the pores and forming a compact mat. With decrease in SL

concentration, lower cell proliferation was observed in case of S3 and S1 scaffolds. The colored background is a result of the matrix staining along with the cells. Fibroblast cells with rounded nuclei were observed throughout the matrix surface suggesting their normal growth on these 3D SF-SL scaffolds (Figure 8b)**.**

Discussion

The present work deals with the development of silk fibroin – sophorolipid hydrogels for use in wound dressing applications and 3D SF-SL scaffolds for tissue engineering applications. We demonstrate that, gelation time of regenerated silk fibroin solution can be considerably reduced from few weeks to few hours by simply mixing it with sophorolipid (biosurfactant) solution. The effective pH of SF-SL solution on mixing was 7.4 ± 0.2. Increasing the SL concentration from 1 w/v% to 3 w/v% resulted in the decrease in gelation time from 189 minutes to 140 minutes. However, further reduction in gelation time could not be achieved even after increasing the concentration of sophorolipid.

The concentration of sophorolipid used in our work is atleast ten times the critical micellar concentration for SL [27]. Thus, as shown in Figure 9 the sophorolipid solution consists of hydrophobic lactonic SL and micelles formed due to SL in acidic form. The lactonic SL is freely available for interaction with silk fibroin. The RSF solution consists of silk fibroin chains with low beta sheet content and small chain entanglements. When this SF solution is added to SL solution, we hypothesize that it results in the formation of mixed micellar particles. These mixed micellar particles are formed due to hydrophobic interactions between SF and acidic SL molecules, whereas the lactonic SL molecules interact with the hydrophobic domains of SF chain. The SF chains therefore assume an extended chain conformation. This leads to hydrophobic interactions between the SF molecules themselves, resulting in the formation of both intra and inter molecular beta sheets. This conformational change in SF drives the formation of a three dimensional gelled network as depicted schematically in Figure 9. The

acidic SL in absence of lactonic SL does not induce gelation of SF (data not shown due to brevity) thus pointing the predominance of hydrophobic interactions between lactonic SL and SF in the process. This corroborates the proposed mechanism and is also in accordance with the mechanism proposed by Wu *et al.* [13] where a surfactant SDS was used to accelerate the gelation of SF solution. However, we are presently conducting further studies to develop a deeper understanding of SF–SL intermolecular interactions at various concentrations and its effect on gelation of silk fibroin.

Sol to gel transition in silk fibroin is marked by conversion of random coil to β-sheet and the ATR-FTIR analysis clearly showed that beta sheet formation is the mechanism of gelation for these solutions. Also, higher concentrations of SL resulted in higher beta sheet contents in the sample. This result implies that the percent *β*-sheet crystallinity in the sample at a given time can be tuned by varying sophorolipid concentration.

These SF-SL hydrogels may be freezed and lyophilised to form 3D scaffolds useful for tissue regeneration. Dry compressive modulus of the 3D scaffolds increases with decrease in SL concentration [11]. The compressive modulus of the SF-SL scaffold with higher percentage of regenerated silk fibroin i.e. S1 sample was found to be maximum.

Cross-sectioned SEM pictographs demonstrated that increasing concentration of sophorolipid leads to development of smaller pore diameters. SF concentration being constant, increasing concentration of SL, leads to the formation of larger number of micelles. Each of these micelle further acts as an interacting site for SF chains which results in higher number of nuclei causing faster gelation and smaller pore sizes. This observation is in agreement with our hypothesis proposed above. In addition, all the SEM images showed no phase separation suggesting homogenous entanglement of sophorolipid and silk fibroin.

Moreover, pore size ranging from 110-350 μm are most favourable for fibrovascular tissue ingrowth due to the balance in two factors, the channel size of sponges for cell infiltration and their surface area for cell attachment [28]. Thus, the pore sizes of resultant 3D scaffold are

expected to support neonatal tissue ingrowth. Also it has already been shown by authors D'britto *et al.* [29] that sophorolipid molecules support and enhance proliferation of cells and our cell culture studies corroborate these findings. The 1 w/v% SL scaffolds show less cell viability as compared to the other scaffolds due to low concentration of SL. With increasing concentration of SL higher cell viability and proliferation could be achieved. Comparison with the pure SF scaffolds could not be accomplished due to its extremely high gelation time thus preventing the formation of consistent and non-contaminated gelled scaffolds.

The present approach of hydrogel fabrication is simple, feasible and requires relatively mild conditions without the employment of any extraneous chemical or cross-linking agent. We consider that such a scaffolding matrix may have immense potential applications in wound dressing and tissue engineering.

Experimental

Regenerated Silk Fibroin solution

Regenerated silk fibroin solutions were prepared from bivoltine *Bombyx mori* cocoons procured from Central Sericultural Research and Training Institute, Mysore, India. The cocoons were boiled in 0.05 w/v% of $NaHCO_3$ (Merck) solution twice for 30 minutes each to remove sericin. The extracted fibroin mass was then dissolved in 9.3 M Lithium Bromide (Sigma Aldrich) solution at 60°C for 4 h. The solution was then extensively dialyzed for 48 h with at least 6 changes of water to ensure complete removal of the salt. The final concentration of Regenerated Silk Fibroin (RSF) solution after dialysis was approximately 5% (w/v) as determined by weighing the remaining solid of a known volume of RSF solution that was dried at 60°C in a vacuum oven. Silk solution with 3% (w/v) concentration was prepared by diluting the 5% solution with deionized water. The pH of the regenerated silk solution was measured to be 6.9 ± 0.2.

Sophorolipid synthesis and solution

Oleic acid derived sophorolipid was synthesized by supplementing *Candida bombicola* (ATCC 22214) with glucose and oleic acid using a method described elsewhere [30]. To determine the effect of sophorolipid concentration on gelation time of RSF, Oleic acid derived sophorolipid solutions were prepared at different concentrations i.e. 1%, 3% and 5% (w/v) respectively. The pH of each concentration solution was adjusted to 8 (±0.2) using 0.1 N NaOH. HPLC chromatogram and FTIR spectrum shown in Figure S1 and S2 in the supporting information confirm the structure of sophorolipid formed.

Formulation of hydrogels and Rheological properties

The purified silk solution of 3 w/v % concentration was mixed with sophorolipid solution at various concentrations (1%, 3% and 5% w/v) in the ratio of 1:1 (v/v) and allowed to stand till gelation. These samples are further referred to as S1, S3 and S5 respectively. To monitor the gelation process and determine the gelation time (GT), rheological measurements of the SF-SL hydrogels were performed using Anton Paar MCR 301 rheometer equipped with Couette flow geometry (CC17). A time sweep experiment was performed at 0.5% strain using a frequency of 6.28 rad/s at 25°C. The experiment was started immediately after mixing the required quantities of SF solution into the pH adjusted SL solution. The cross-over of G′ and G″ was considered to be the gelation time.

Fourier transformed Infrared Spectroscopy (FTIR)

The gelation of the SF-SL solutions was also investigated using Fourier Transformed Infrared Spectroscopy (Protégé 460, Nicolet, USA), employing a horizontal Attenuated Total Reflectance (ATR) ZnSe cell. After mixing SL to SF, the solution was drop casted on ZnSe cell and spectrum was measured. As the gelation progressed the gels were loaded for IR measurements. The FTIR spectrum in the amide I region (1580-1720cm^{-1}) was deconvoluted using the Peakfit v

4.12 software. The spectrum was corrected for baseline using a linear two-point method. A second derivative method was used to identify the peaks and the spectrum was smoothened till 12 peaks (1595–1605, 1605-1615, 1616-1621, 1622-1627, 1628-1637, 1638-1646, 1647-1655, 1656-1662, 1663-1670, 1671-1685, 1686-1696, 1696-1703 cm^{-1}) could be fit. These peak positions have been defined by Hu et al. [24]. A Gaussian fit with fixed peak width was used for automatic curve fitting and the spectrum was deconvoluted into 12 peaks. The % beta sheets was then calculated as the sum of % area under the four beta sheet peaks (1616-1621, 1622-1627, 1628-1637, 1696-1703 cm^{-1}).

Preparation of scaffolds:

The SF-SL solutions were allowed to gel in a 96 well cell culture plate at room temperature. The cell culture plate was then immersed in Liquid Nitrogen for 30 minutes. This frozen plate was then stored in -80°C freezer overnight and the plate was lyophilized for 16-20 h, to obtain 3D SF-SL porous scaffolds.

Measurement of dry compression modulus

Dry compression modulus measurements were performed on an MCR 301 Anton Paar rheometer using 8mm parallel plate geometry. Cylindrical scaffolds of approximately 5mm diameter and 5mm height were used for the measurement. A cross-head displacement speed of 5µm/s was used to displace the top plate and the normal force was measured. At least 3 samples per measurement were recorded. A graph of stress *vs* strain was then manually plotted and the dry compression modulus was determined to be the slope of initial linear region in the plot.

Scanning Electron Microscopy

The cross-sectional morphology of the prepared scaffolds was observed using the scanning electron microscope (Quanta 200 3D, FEI), with an accelerating voltage of 15 kV. Cut section of

the scaffolds was mounted on aluminum stubs and coated with a thin layer of gold to prevent charging. Representative images of each sample were captured at suitable magnifications.

Cell Culture

Cell proliferation activity was determined in mouse fibroblast cell line L929 (ATCC CCL-1) obtained from National Center for Cell Science, Pune. The mouse fibroblast of adherent nature (L929) was routinely cultured and maintained at 37^{o}C with 5% CO_2 in DMEM (Gibco, Invitrogen) supplemented with 10% fetal bovine serum (FBS; Gibco 10082-139). The culture medium was replaced every 2 days.

Fibroblast seeding and culture on porous scaffolds

The scaffolds were autoclaved and UV sterilized for 25 min before any cell culture study. Adherent fibroblasts were permitted to achieve 90% confluence. Cells were harvested in log phase using trypsin (0.05% trypsin, 0.02% EDTA, in PBS). The cell counts were performed by haemocytometry. The cell suspensions were diluted in DMEM medium to obtain the cell density of $1x10^4$ cells/mL. An aliquot of 100 µL of each suspension was seeded in a drop-wise manner on the top of the sterilized scaffolds disc in 96-well cell culture plates. The plate was then left undisturbed at 37°C in an atmosphere of 5% CO_2 and 95% relative humidity in a CO_2 incubator. The culture medium was replaced every 2 days.

Cell adhesion assay

For cell adhesion assay, the cells were seeded in 96 well plate on top of the sterilized scaffold disc and incubated in a humidified atmosphere with 5% CO_2 at 37°C as mentioned above. At 4 and 8 h, the cells were gently harvested in 100 µL PBS at pH 7.4 and then counted using a haemocytometer. By subtracting the number of washed out fibroblasts from $1x10^4$ cells per scaffold, the number of cells remained adhering to each scaffold disc was calculated (Equation 1).

(1x10^{4}cells per scaffold - number of washed out L929 fibroblast cells) = Number of cells adhering to each scaffold *(Equation 1)*

Cell proliferation assay to study the metabolic activities of cells within scaffolds

MTT (3-(4,5-dimethylthiazol-2-yl)-2,5- diphenyltetrazolium bromide, Sigma Aldrich) assay was performed to quantify the proliferation of L929 fibroblast cells within the constructs (scaffolds with cells) at intervals of 2, 4 and 7 days. The *in vitro* cytotoxic effect of the fabricated scaffold was investigated by a standard MTT assay, a widely adopted method of measuring cellular proliferation as described elsewhere [31,32]. The scaffolds were sectioned to disc weighing approximately 1.5 mg ± 0.2 and used for all cell culture studies. A 100 µL suspension of 1x10^4 cells/mL was seeded on sterilized scaffold disc kept in 96-well cell culture plates. The plates were then left undisturbed at 37°C in an atmosphere of 5% CO_2 and 95% relative humidity within a CO_2 incubator. At the end of the incubation, the suspensions containing the unattached cells was discarded and each well containing the scaffold and attached cells was washed thrice with 1 mL of PBS. 0.01 ml MTT (5 mg/mL in phosphate-buffered saline) was then added in each well. After 4 h of incubation at 37°C, the formazan product was solubilized by the adding 0.2 mL of 0.04 N HCl in isopropanol. Optical density was measured on a SPECTRAmax PLUS 384 plate reader (Molecular Devices Inc, USA), at 570 nm. The assay was carried out with only MTT solution as negative control and cell suspension as positive control. All experiments were performed in triplicates, and the quantitative value was expressed as the average ± standard deviation.

Confocal microscopy

The morphology of the adhered cells on constructs (cell laden scaffold disc) was studied using a Thermo Scientific™ ArrayScan™ XTI High Content Analysis (HCA) Reader. After incubation for 24 hours the cell laden scaffold discs were washed thrice with PBS (pH 7.4) and incubated in 4% paraformaldehyde for 25 minutes to fix the constructs. For fluorescence microscopic study,

the fixed constructs were stained with 1 μM DAPI (4',6-Diamidino-2-Phenylindole, Sigma) and 1 μM Nile red (Sigma). For staining, 100 μL dye solutions (prepared in DMSO) were mixed with the cell suspension (9.9 mL) and kept at room temperature for 30 minutes in dark. The cells were then washed thrice before acquiring images. The images were acquired using a confocal laser-scanning microscope as 4X4 binning with a 20X objective (Olympus FV1000). The 3D multichannel-image processing was done using Thermo Scientific™ HCS Studio™ 2.0 Cell Analysis Software.

Conclusion

The accelerated gelation of silk fibroin is achieved in this investigation by a simple method that involves addition of sophorolipid, a biosurfactant solution. We demonstrated here that the addition of sophorolipid reduces the gelling time of SF solutions from few weeks to few hours. These SF-SL hydrogels can be further lyophilized to form 3D scaffolds. The compression modulus and pore size of the scaffolds can be very easily tuned by controlling the SL concentration. We also showed that L929 cells adhered and proliferated on these constructs. The SF-SL hydrogels will find applications in wound dressing while the SF-SL 3D scaffold may have potential use in tissue regeneration.

Acknowledgements:

This work is financially supported by the Council of Scientific and Industrial Research, New Delhi, India and the 12th Five Year Plan project CSC00134 titled "Molecules to Materials to devices". Authors would like to thank Ms. Chaitali Deshpande for her help during rheological measurements.

References:

1 C. Vepari and D. L. Kaplan, *Progress in Polymer Science (Oxford)*, 2007, 32, 991–1007.

2 S. Rammensee, D. Huemmerich, K. D. Hermanson, T. Scheibel and A. R. Bausch, *Applied Physics A: Materials Science and Processing*, 2006, **82**, 261–264.

3 L. Yu and J. Ding, *Chemical Society reviews*, 2008, **37**, 1473–1481.

4 B. Balakrishnan and R. Banerjee, *Chemical Reviews*, 2011, 111, 4453–4474.

5 L. Wang, Y. Wang, J. Qu, Y. Hu, R. You and M. Li, *Journal of Biomaterials and Nanobiotechnology*, 2013, **04**, 213–221.

6 T. Yucel, P. Cebe and D. L. Kaplan, *Biophysical Journal*, 2009, **97**, 2044–2050.

7 X. Wang, J. A. Kluge, G. G. Leisk and D. L. Kaplan, *Biomaterials*, 2008, **29**, 1054–1064.

8 G. G. Leisk, T. J. Lo, T. Yucel, Q. Lu and D. L. Kaplan, *Advanced Materials*, 2010, **22**, 711–715.

9 T. Yucel, N. Kojic, G. G. Leisk, T. J. Lo and D. L. Kaplan, *Journal of Structural Biology*, 2010, **170**, 406–412.

10 A. Matsumoto, J. Chen, A. L. Collette, U. J. Kim, G. H. Altman, P. Cebe and D. L. Kaplan, *Journal of Physical Chemistry B*, 2006, **110**, 21630–21638.

11 U. J. Kim, J. Park, C. Li, H. J. Jin, R. Valluzzi and D. L. Kaplan, *Biomacromolecules*, 2004, **5**, 786–792.

12 G.-D. Kang, J.-H. Nahm, J.-S. Park, J.-Y. Moon, C.-S. Cho and J.-H. Yeo, *Macromolecular Rapid Communications*, 2000, **21**, 788–791.

13 X. Wu, J. Hou, M. Li, J. Wang, D. L. Kaplan and S. Lu, *Acta Biomaterialia*, 2012, **8**, 2185–2192.

14 Nagarkar. S, and Lele. A, US Patent No. 8779097 B2, 2014.

15 J. A. Casas and F. García-Ochoa, *Journal of Bioscience and Bioengineering*, 1999, **88**, 488–494.

16 M. Kjellin and I. Johansson, *Surfactants from Renewable Resources*, 2010.

17 V. Dengle-Pulate, P. Chandorkar, S. Bhagwat and A. A. Prabhune, *Journal of Surfactants and Detergents*, 2013, **17**, 543–552.

18 V. Shah, G. F. Doncel, T. Seyoum, K. M. Eaton, I. Zalenskaya, R. Hagver, A. Azim and R. Gross, *Antimicrobial Agents and Chemotherapy*, 2005, **49**, 4093–4100.

19 J. Chen, X. Song, H. Zhang and Y. Qu, *Enzyme and Microbial Technology*, 2006, **39**, 501–506.

20 K. Joshi-Navare, A. Shiras and A. Prabhune, *Biotechnology Journal*, 2011, **6**, 509–512.

21 F. Borzeix, and R. Malmaison, US006057302A, 2000.

22 K. Joshi-Navare and A. Prabhune, *BioMed Research International*, 2013, **2013**.

23 S. Nagarkar, A. Patil, A. Lele, S. Bhat, J. Bellare and R. A. Mashelkar, *Industrial and Engineering Chemistry Research*, 2009, **48**, 8014–8023.

24 X. Hu, D. Kaplan and P. Cebe, *Macomolecules*, 2006, **39**, 6161–6170.

25 E. S. Gil, J. A. Kluge, D. N. Rockwood, R. Rajkhowa, L. Wang, X. Wang and D. L. Kaplan, *Journal of Biomedical Materials Research - Part A*, 2011, **99 A**, 16–28.

26 B. Kundu and S. C. Kundu, *Biomaterials*, 2012, **33**, 7456–7467.

27 R. D. Ashby, D. K. Y. Solaiman and T. A. Foglia, *Biotechnology Letters*, 2008, **30**, 1093–1100.

28 M. Yamamoto, Y. Tabata, H. Kawasaki and Y. Ikada, *Journal of Materials Science: Materials in Medicine*, 2000, **11**, 213–218.

29 V. D'Britto, H. Kapse, H. Babrekar, A. A. Prabhune, S. V Bhoraskar, V. Premnath and B. L. V Prasad, *Nanoscale*, 2011, **3**, 2957–2963.

30 I. N. A. Van Bogaert, K. Saerens, C. De Muynck, D. Develter, W. Soetaert and E. J. Vandamme, *Applied microbiology and biotechnology*, 2007, **76**, 23–34.

31 G. Ciapetti, E. Cenni, L. Pratelli and A. Pizzoferrato, *Biomaterials*, 1993, **14**, 359–364.

32 T. Mosmann, *Journal of immunological methods*, 1983, **65**, 55–63.

Graphical Abstract

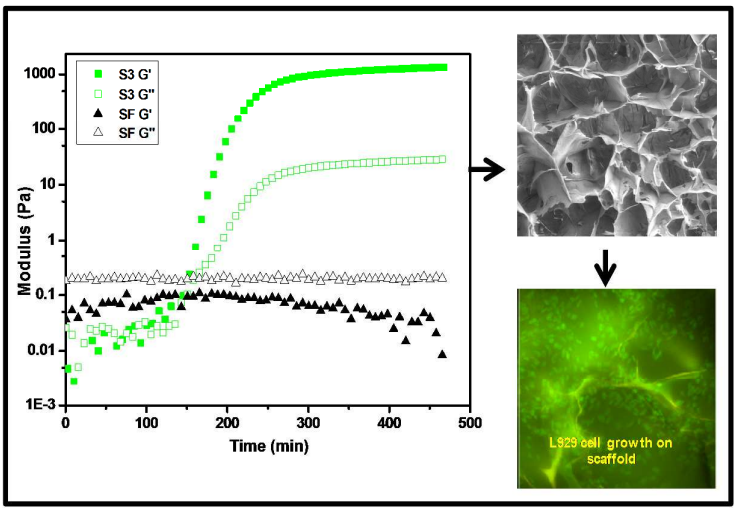

Textual abstract

Faster gelation of silk fibroin using biosurfactants: sophorolipid, towards 3D scaffolds for biomedical application

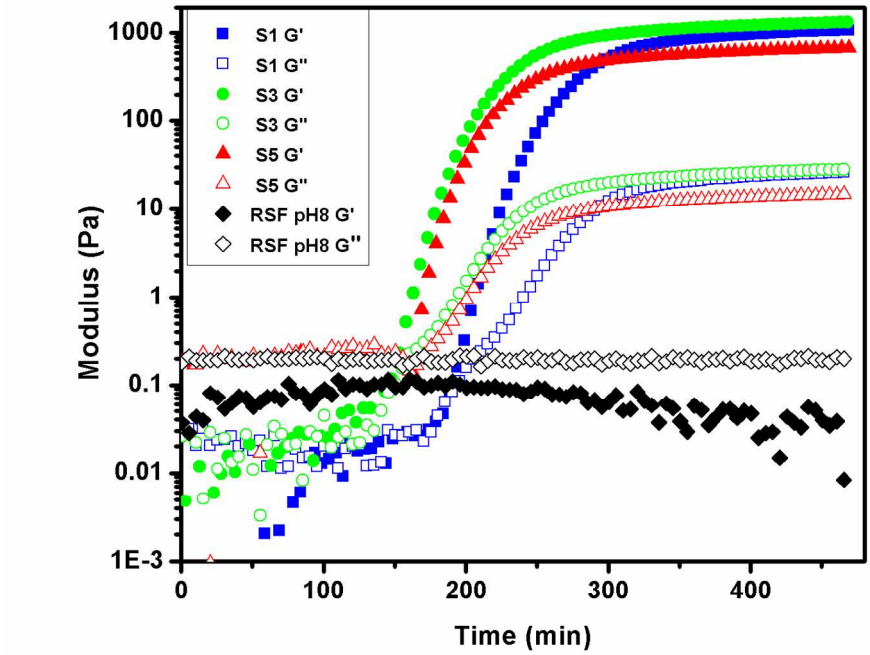

Figure 1: Time sweep rheology experiments on pure SF, S1, S3 and S5 samples
279x215mm (150 x 150 DPI)

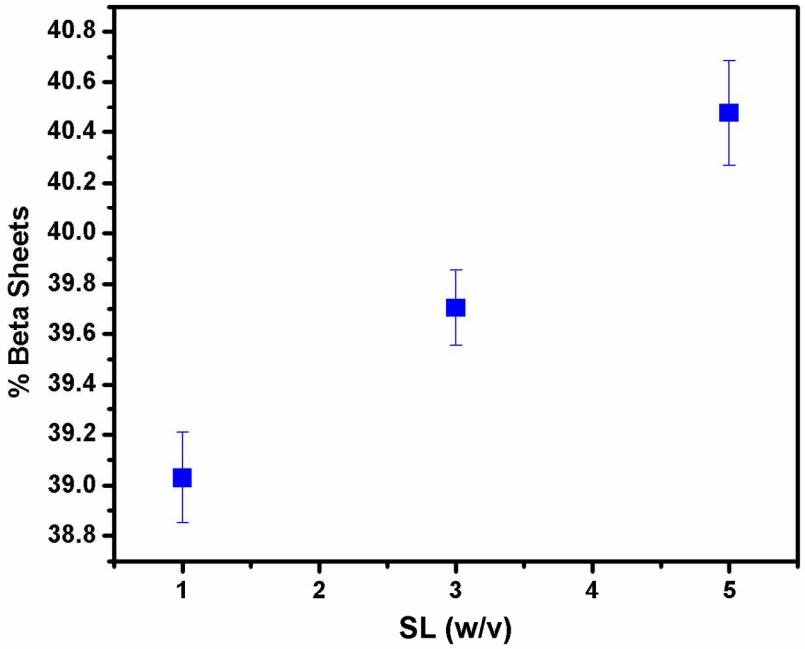

Figure 3: % Beta sheets of SF+SL hydrogel for S1, S3 and S5 samples
279x215mm (150 x 150 DPI)

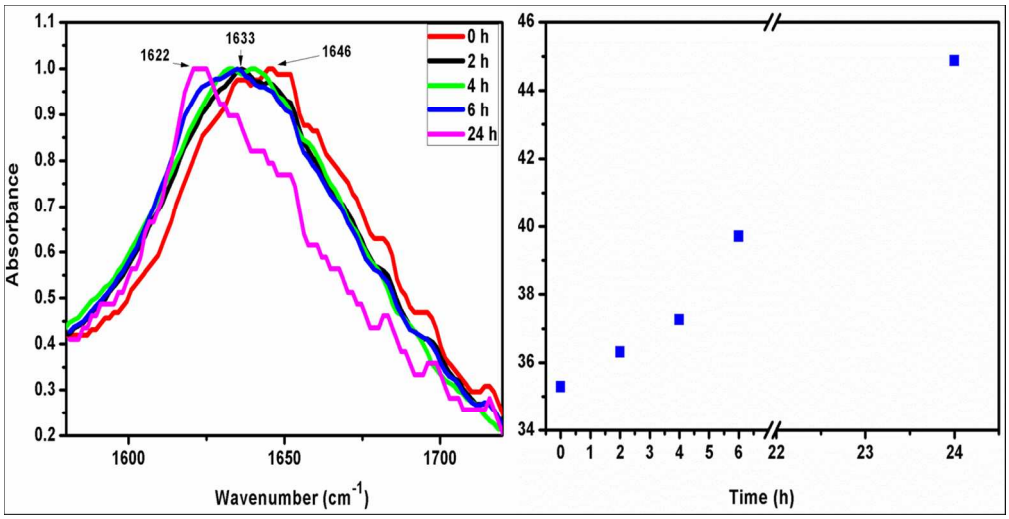

Figure 2: (a) ATR–FTIR spectra of S3 solution as a function of time (b) % beta sheet change in S3 as a function of time after amide I peak deconvolution
244x124mm (150 x 150 DPI)

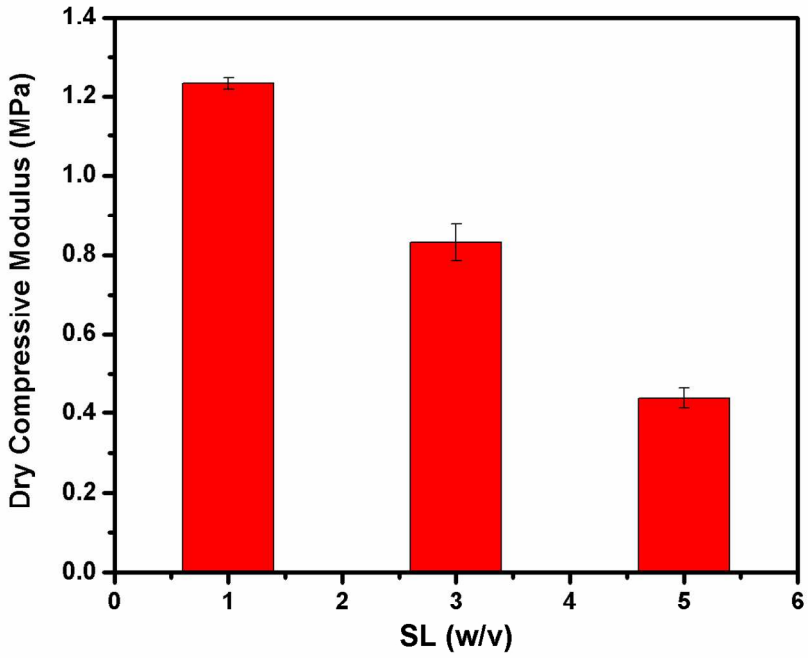

Figure 4: Compressive modulus of SF+SL hydrogel as a function of SL concentration (i.e. 1%, 3% and 5% (w/v)) at 25 °C.
279x215mm (150 x 150 DPI)

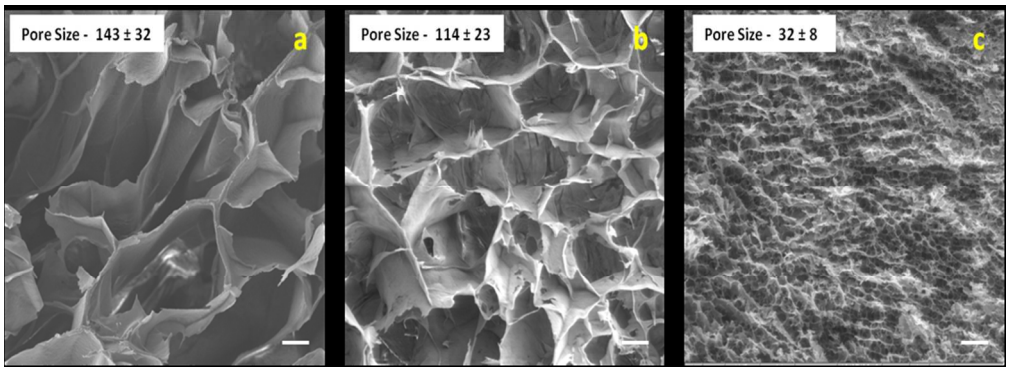

Figure 5: Scanning electron micrographs of cut surface of lyophilized scaffolds for (a) S1, (b) S3 and (c) S5 samples. Scale bar for all images is 50μm
187x78mm (150 x 130 DPI)

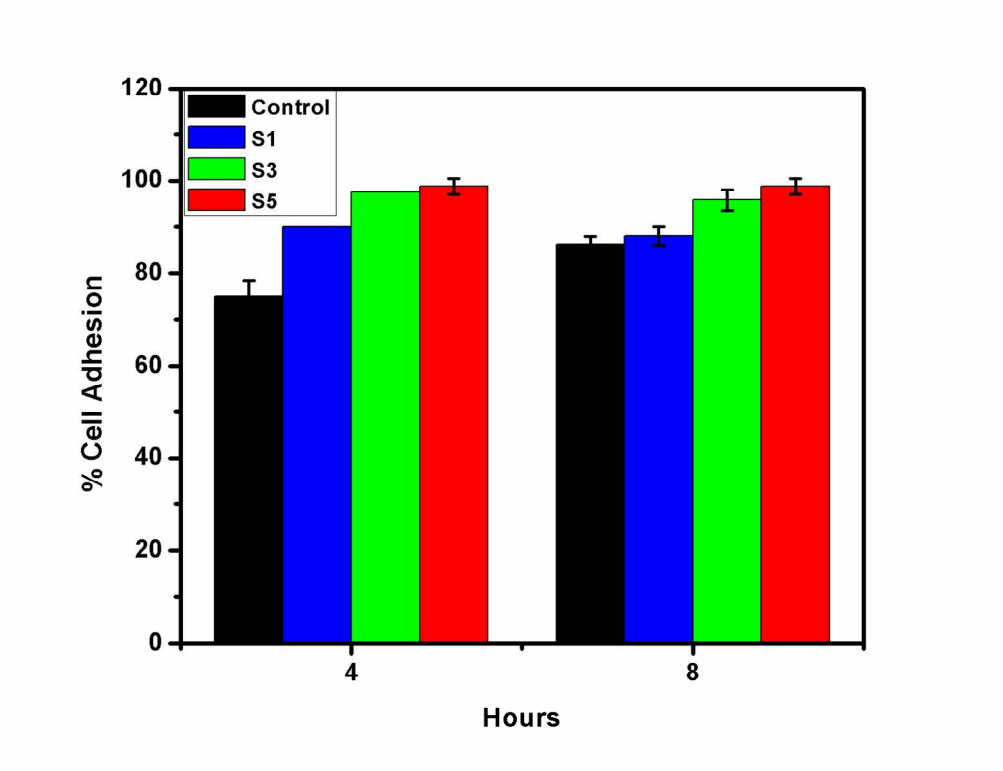

Figure 6: Adhesion of Mouse fibroblast (L929) cells as a function of time on lyophilized scaffolds prepared using S1, S3 and S5 solutions
279x215mm (150 x 150 DPI)

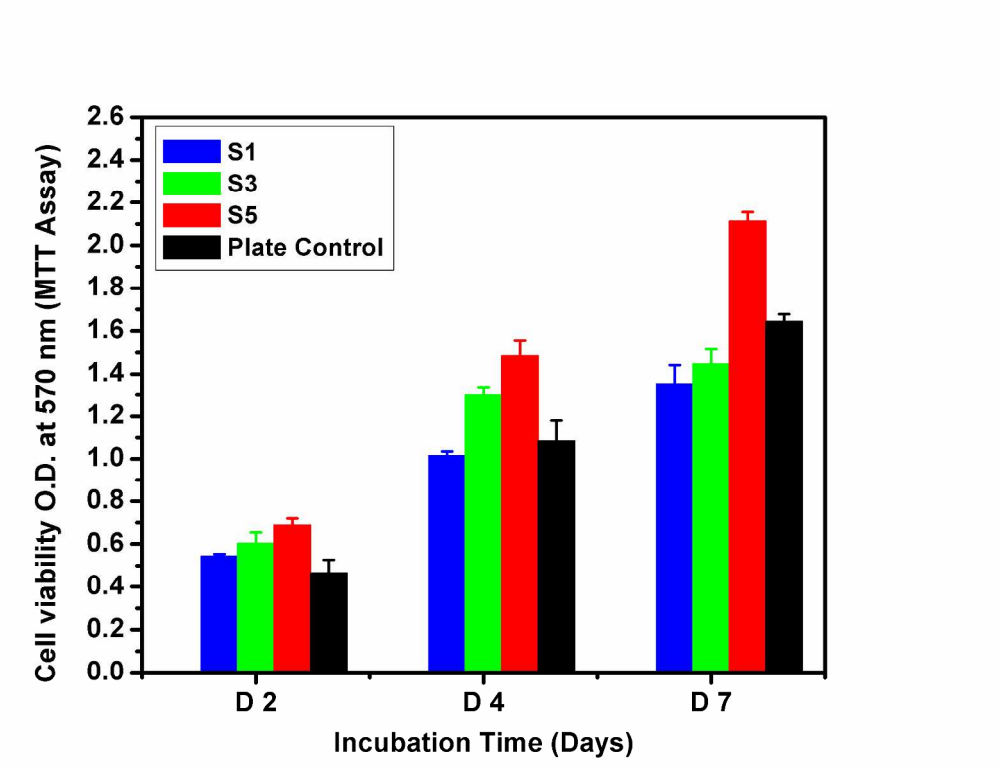

Figure 7: MTT assay showed that fibroblasts exhibited high metabolic activity cultured on three dimensional scaffold matrices for up to 7 days.
279x215mm (300 x 300 DPI)

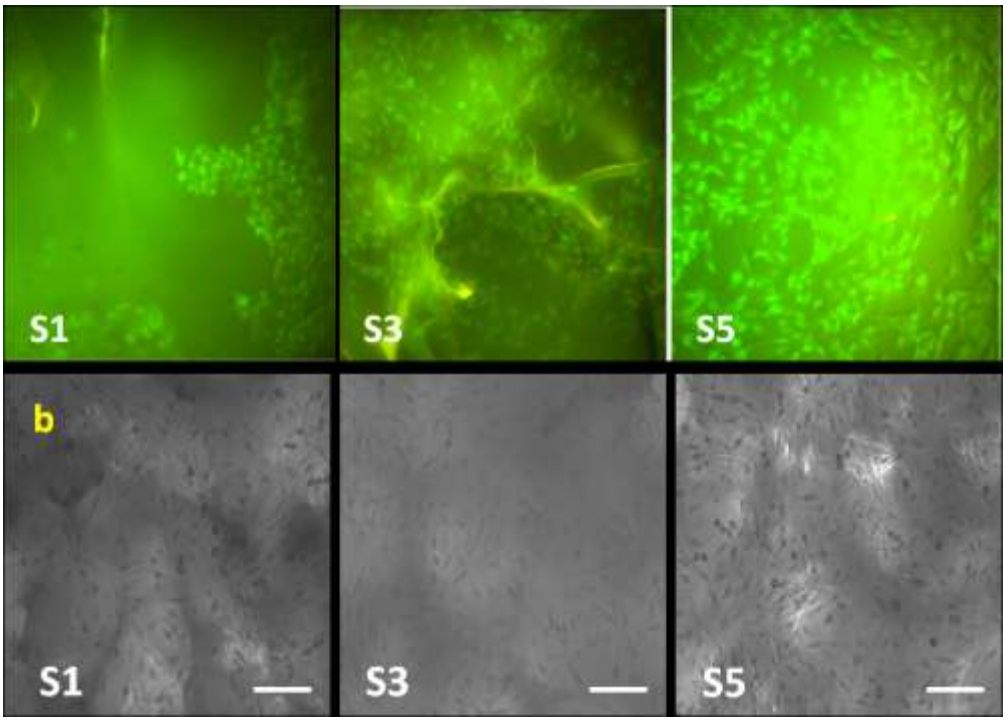

Figure 8: (a) Confocal images of DAPI and Nile red stained L929 fibroblast cells and scaffold matrices. (b) Adherent cell morphology on scaffolds 48 h post seeding and fixing with 2.5 % glutaraldehyde using Floid® Cell Imaging System with fixed 20X Plan Fluorite objective having Image resolution - 1296 x 964 pixels. Scale bar for all images is 100 µm.
158x112mm (150 x 150 DPI)

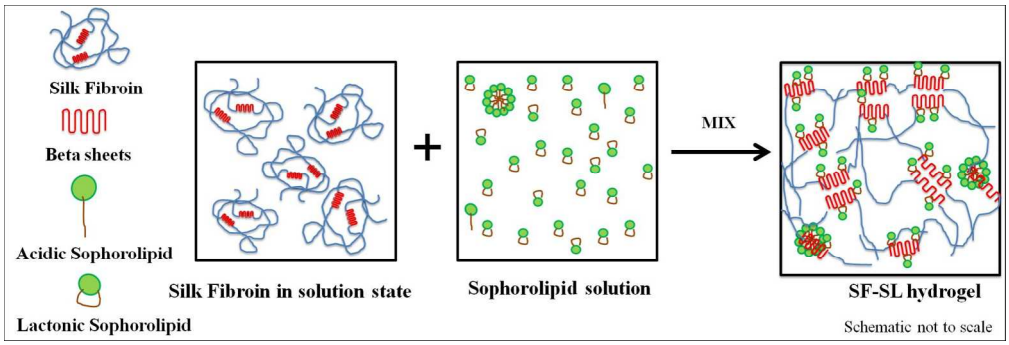

Figure 9: Schematic depicting proposed mechanism of SF-SL gelation.
400x166mm (126 x 102 DPI)